

Photoemission of a doped Mott insulator: spectral weight transfer and qualitative Mott-Hubbard description

M. Sing, S. Glawion, M. Schlachter, M. R. Scholz, K. Goß, J. Heidler, G. Berner, and R. Claessen
Experimentelle Physik 4, Universität Würzburg, Am Hubland, D-97074 Würzburg, Germany
 (Dated: November 2, 2018)

The spectral weight evolution of the low-dimensional Mott insulator TiOCl upon alkali-metal dosing has been studied by photoelectron spectroscopy. We observe a spectral weight transfer between the lower Hubbard band and an additional peak upon electron-doping, in line with quantitative expectations in the atomic limit for changing the number of singly and doubly occupied sites. This observation is an unconditional hallmark of correlated bands and has not been reported before. In contrast, the absence of a metallic quasiparticle peak can be traced back to a simple one-particle effect.

PACS numbers: 79.60.-i,71.27.+a,71.10.Fd

The question how the electronic structure of a Mott insulator [1] develops upon doping is a long-standing problem in condensed matter physics. Marked additional attention is lent to this issue by the fact that the cuprate high-temperature superconductors are doped Mott (or charge-transfer) insulators as well [2]. In Mott insulators, short-range electron correlations induce a charge gap in the single-particle excitation spectrum for partially occupied bands with integer filling, whereas band theory predicts a metal. For transition-metal oxides, the local (onsite) Coulomb energy U can be defined as the energy difference for removing and adding an electron to a site with the initial occupancy d^n , i.e., with n electrons in the d shell. The corresponding single-particle excitation energies give rise to the incoherent spectral weight of the lower (LHB) and upper Hubbard bands (UHB), respectively. At room temperature, TiOCl is a prototypical low-dimensional Mott insulator with a $3d^1$ configuration [3, 4]. In this respect it represents the electron analogue to the cuprates whose undoped parent compounds have a single hole in the $3d$ shell.

Upon electron doping by alkali-metal evaporation [5] we find in photoemission spectra a benchmark case of what is known under the notion of spectral weight transfer (SWT), a phenomenon, which uniquely discriminates systems of independent electrons from those where electron correlations are important [6]. Such kind of SWT has previously been observed in x-ray absorption spectroscopy (XAS) on hole-doped cuprates; there is still an active debate going on if the peculiar behavior of the SWT in overdoped samples signals a different nature or strength of correlations in this regime [7–9]. However, the SWT observed there does not represent a canonical case since electrons are doped essentially into the O $2p$ states and SWT is only introduced via hybridization of the intrinsically *non*-correlated O $2p$ with the correlated Cu $3d$ states. In addition, XAS — even at the O K edge — is not a clean electron-addition spectroscopy due to excitonic effects. In contrast, we can observe in TiOCl with its d^1 configuration the SWT for the first time di-

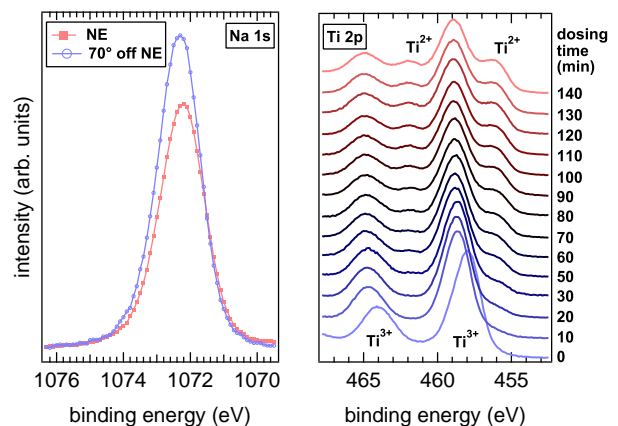


FIG. 1. (Color online) Left: Na $1s$ spectra at normal emission (NE) and at an angle $\theta = 70^\circ$ off normal emission. Right: Ti $2p$ spectra for various Na vapor dosing times.

rectly in the photoemission electron-removal spectra of the Ti $3d$ states over a wide doping range. That we do not detect a metallic phase at any doping concentration up to $x \approx 0.4$ can be traced back to a single-particle, electrostatic alloy effect.

TiOCl crystallizes in a two-dimensional (2D) structure, where Ti-O bilayers are stacked along the c -axis and only weakly interact through van-der-Waals forces, which leaves space in between for intercalation with dopants. With the Ti ions centered in a distorted octahedron of O and Cl ligands, the degeneracy of the $3d$ - t_{2g} orbitals is lifted such that the lowest d orbitals are split by about 0.3 eV. Single crystals were grown by chemical vapor transport as described elsewhere [10]. Clean surfaces were exposed by *in situ* cleavage and dosed by alkali-metal vapor from SAESTM dispensers. Data was recorded with a SPECS PHOIBOS 100 analyzer at a total energy resolution of 700 meV and 70 meV using Al K_α (1486.6 eV) and He I_α (21.22 eV) radiation for core-level (XPS) and valence-band (UPS) spectroscopy, respectively. To minimize charging and to ease atomic diffusion the samples were held at elevated temperatures

(≈ 360 K) during dosing and measurements. Preservation of symmetry and atomic long-range order at the surface were monitored by low-energy electron diffraction (LEED), while the chemical stability of the oxygen was inferred from the unchanged O $1s$ core-level spectra and a stoichiometric analysis of the Ti : O ratio [11].

That dosing the TiOCl crystals by alkali-metal vapor (Na and K; within the scope of this study, both are interchangeable) essentially leads to both intercalation of the alkali-metal atoms into the van-der-Waals gaps and the donation of electrons to the Ti sites — as is known from the structurally identical TiNCl [12] — is demonstrated in Fig. 1. In the left panel, the Na $1s$ core-level spectrum is displayed for normal emission (NE) and an emission angle of 70° with respect to the surface normal. If the alkali-metal atoms only built an overlayer without intercalating into the TiOCl structure, one would expect a small and a huge Na $1s$ signal at NE and 70° , representing bulk and surface sensitive spectra, respectively. However, both signals are of comparable intensity. Actually, the moderately higher intensity at 70° can be quantitatively understood if one simulates the PES signal [13] due to the discrete vertical distribution of the Na ions, taking into account the stronger exponential damping of photoelectrons emitted deeper from the solid. A direct spectroscopic proof for successful electron *doping* can be inferred from the Ti $2p$ core-level spectra in the right panel of Fig. 1. The spectral weight at the lower binding energy sides of the Ti $^{3+}$ related main doublet, which increases with dosing time, can be attributed to emission from the $2p$ level of Ti $^{2+}$ as evidenced by its chemical shift of 2.7 eV and thus is a direct manifestation of extra electrons at the Ti sites. Moreover, from a standard fitting procedure using two Voigt profiles for each Ti valency to the Ti $2p$ spectra (cf. [11]) a rather accurate determination of the electron doping concentration can be obtained through $x = A(2+)/[A(2+) + A(3+)]$, where A denotes the area of the Voigt profiles for each valency.

In the angle-integrated UPS spectra of the valence band (see Fig. 2; spectra corresponding to those of Fig. 1, right panel), the successful electron doping manifests itself in additional spectral weight, piling up with increasing doping concentration x near the chemical potential μ_{exp} [14]. Already after a tiny amount of dosing the whole spectrum shifts by about 0.6 eV to higher binding energies. In the most simple picture of a Mott insulator the abrupt shift corresponds to a jump of the chemical potential from the midgap position to the lower edge of the UHB [15]. Note that the observed value of 0.6 eV is much smaller than half the optical gap of undoped TiOCl, which is ≈ 2 eV. In addition, with further doping one would expect the formation of a coherent quasiparticle peak at the chemical potential concomitant with a decrease of the LHB (and UHB) spectral weight, indicating a strongly correlated metallic state [16]. In-

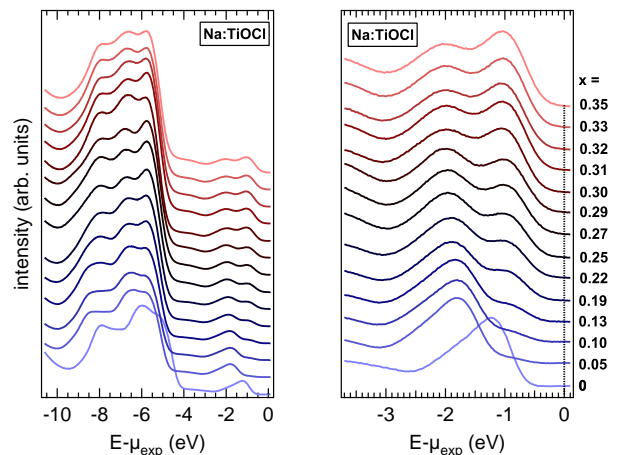


FIG. 2. (Color online) Evolution of the overall valence band spectra (left) and the Ti $3d$ spectral weight near the chemical potential (right) as a function of electron doping x .

stead, the doping-induced spectral weight develops in a broad hump, partly overlapping with the original spectral weight of the LHB. As we will see later, the latter two observations, the inconsistent gap value and the absence of a quasiparticle peak, can be explained by a simple single-particle effect.

What is more remarkable, though more inconspicuous at first glance is the development of the relative spectral weight of the two peaks at the chemical potential. If one normalizes the integral $3d$ part of the spectra to $1 + x$ in accordance with the conservation of spectral weight, one finds that the doping-induced weight apparently grows at the expense of the LHB. A quantitative analysis by fitting two Gaussian to the spectra after subtraction of a Shirley background (cf. [11]) reveals that indeed the LHB spectral weight decreases as $1 - x$ while the weight of the additional band increases as $2x$ (see Fig. 3 (a) for K intercalation).

In case of a semiconductor, one would expect that the additional weight upon doping increases just like x , meaning that the extra electrons are hosted by the formerly unoccupied conduction band. In this case, the electronic structure remains essentially unaffected by the addition of electrons, merely the band states are successively filled up. In sharp contrast, at its core, electron correlations means that the electronic structure depends on the actual local occupancy (of the correlated states) at each site, not only on the mean occupancy. Hence, each additional electron in the $3d$ shell will change the entire $3d$ single-particle excitation spectrum. This can be easily seen in a local picture with no hopping ($t = 0$) between neighboring sites, i.e., when no quasiparticle is present [6]. In this case, for each additional electron donated to the Ti $3d$ states, one possibility to remove an electron from a singly occupied Ti site at an orbital energy ε is discarded in favor of two possibilities to remove

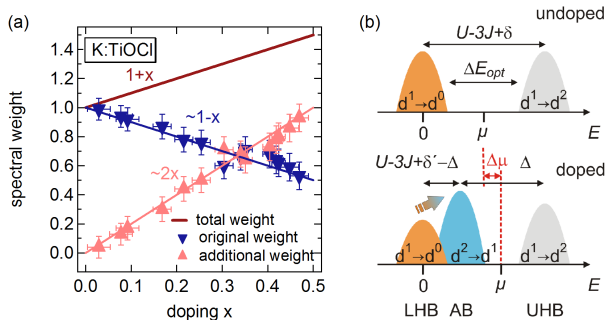


FIG. 3. (a) (Color online) Quantitative analysis of the SWT in the Ti $3d$ states upon doping. (b) (Color online) Sketch of the spectral weight distribution for TiOCl in the undoped and doped case. The arrow symbolizes the SWT. For details see text.

an electron from a doubly occupied site, where correlations are important. Due to the local Coulomb repulsion U , the single-particle removal will happen at an energy $\varepsilon + U$. This SWT is exactly what we observe here. We emphasize that the SWT is the most direct way to monitor correlation effects experimentally since it straightly reflects the change of the electronic structure connected with the local electron occupancy.

If finite hopping with amplitude t is admitted, the SWT will be even faster than $2x$ [6], which we do not find. This suggests that alkali-metal intercalated TiOCl lies in the strong-coupling regime which seems conceivable, facing U/t values as reported from density functional calculations of the order of 20 [4, 17]. Partly, the canonic $2x$ behavior might also be a consequence of the disorder potential, induced by the intercalated alkali-metal ions, which may hinder the electron hopping.

In any case, at this stage it is manifest that a simple Hubbard picture in the atomic limit provides the correct basis to explain the SWT as the most salient feature of our data, while it obviously has to be refined to account also for the other observations, in particular the insulating behavior at all doping levels. A steer in the right direction might come from recent combined molecular dynamics and density-functional calculations for Na intercalated TiOCl which also find insulating behavior upon doping [18]. As effective single-particle calculations they — by definition — cannot account for the SWT in our data. However, in this study in-gap d states below the chemical potential show up upon doping, which are located at those Ti sites in the immediate vicinity of Na ions and host the extra electrons. This result may be taken as a hint that single-particle effects are responsible for the persistent insulating character despite doping.

In the following, we seek to include one-particle effects of that kind on top of a Hubbard model description to fully account for all the features of our data. We start by assuming that in n-doped TiOCl the energy at Ti sites with an alkali-metal ion next to them will be lowered due

to its associated Coulomb potential by an amount Δ . It is thus the alkali-metal ions themselves that create sites with modified single-particle energies to which they donate their electrons (we call these second kind of Ti sites electrostatically induced alloy sites, which give rise to an alloy band, AB). Starting doping at half-filling, for any $x < 1$ the system will be insulating since on the one hand all pristine Ti sites are singly occupied (corresponding to a Mott insulator) while all alloy Ti sites are doubly occupied (corresponding to a band insulator). Note that no doping into the UHB is achieved and hence it remains above the chemical potential, being invisible in photoemission. The spectral weight distribution for both the doped and undoped case is sketched in Fig. 3 (b). Each feature (LHB, UHB, AB) is labelled with the corresponding single-particle excitation by denoting the d configurations of the initial and final states. In this picture, the SWT now occurs from the LHB to the AB which as being due to doubly occupied sites takes over the role of the UHB in a clean (and local) Mott-Hubbard picture.

Our arguments can be corroborated quantitatively. In a multi-orbital Hubbard model in the atomic limit, i. e., $t = 0$, with degenerate orbital energies and only one sort of sites an extra electron will be hosted in a second orbital with parallel spin due to the gain in intraatomic exchange energy. Hence, the separation of the LHB and UHB is given by $U - 3J$, where J is the Hund's rule coupling [19, 20]. Taking a small difference δ in orbital energies into account ($\delta \ll J$), the separation is given by $U - 3J + \delta$ (cf. upper half of Fig. 3 (b)). From optical absorption [21] it is known that the charge gap is about 2 eV. In the doped case, the position of the LHB and UHB remain essentially unchanged, since the alkali-metal ions hardly affect the orbital energies of remote Ti sites [18]. Instead, the AB emerges within the original charge gap below the chemical potential owing to the lowered orbital energies at Ti sites next to the alkali-metal ions. From the PES data, its energy separation from the LHB amounts to ≈ 1 eV. Note that in addition to the electrostatic potential Δ also the crystal-field splitting between the ground state orbital and the next higher orbital is slightly lowered from ≈ 0.3 eV to ≈ 0.1 eV according to the density-functional calculations in Ref. 18. Hence, in the atomic limit, the separation between LHB and AB may be expressed as $U - 3J + \delta' - \Delta$. From the sketched qualitative picture the chemical potential lies in midgap position between AB and UHB. With the 1 eV splitting between LHB and AB it follows that the chemical potential in the doped case will jump by about 0.5 eV with respect to the undoped case in agreement with the PES data. Moreover, with reasonable assumptions for $U - 3J$ of 2.5 – 3.5 eV [18, 19, 22], one can estimate the potential Δ at the alloy sites to be ≈ 2 eV. This value can be understood in a simple point charge model. With the relaxed crystal structure from Ref. 18 for one Na atom per four unit cells, the Na ion induced Coulomb potential at the next Ti site is about

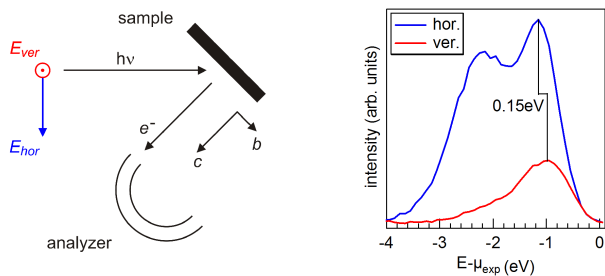


FIG. 4. (Color online) Geometry and PES spectra of polarization-dependent measurements. An independent component analysis allows a quantitative determination of the crystal-field splitting at a doubly occupied site.

2 eV, taking screening by a dielectric constant around 3.5 [23] into account, and thus well compares with the value derived from our model.

Above, the lifted degeneracy of the two lowest d orbitals in TiOCl was only taken into account for the sake of formal correctness. It adds only a negligible inaccuracy to an estimation of the model parameter Δ . This splitting in the orbital energies of ≈ 0.1 eV according to theory [18] apparently cannot be resolved in the AB related feature of the PES spectra in Fig. 2 due to its intrinsic broadness. However, one can exploit the different symmetry of these two orbitals with respect to the (b, c) crystal mirror plane to switch between them in PES by changing the polarization of the incoming photons from horizontal to vertical using the geometry sketched in Fig. 4 [22]. From the different orbital symmetries, one would expect to be able to switch between the LHB and one component of the AB at lower energy, and another component of the AB at ≈ 0.1 eV higher energy, which then would reveal the multi-orbital character of this “band”. It is important to understand that this multi-orbital effect is due to the fact that — in the language of PES — after removing an electron from a doubly occupied alloy site the remaining electron might occupy the one or the other orbital (all other orbital degrees of freedom are quenched) with different energies. It must not be thought of in terms of single-particle states which are occupied in the initial ground state.

The result of this experiment is depicted in Fig. 4. Shown are the curves resulting from an independent component analysis, since due to the finite degree of polarization, a possible small misalignment of the sample, and symmetry-breaking phonons, for one polarization also a certain fraction of the spectrum for the other is monitored

and *vice versa*. The unspoilt spectra indeed show the expected behavior and allow to infer an energy splitting of the orbitals contributing to the AB of about 0.15 eV.

In summary, we have found by photoelectron spectroscopy a prime example for the spectral weight transfer upon doping in a prototypical Mott insulator, which is *the* fingerprint of many-body physics. On the other hand, the persistent insulating character of TiOCl at all doping levels is identified as a single-particle effect on top of the many-body physics. Both the single-particle and the many-body aspects can be reconciled within an accordingly adapted Hubbard model description. A full quantitative account of our results calls for sophisticated calculation schemes which combine *ab initio* density-of-states and many-body methods. Our data provide a benchmark for such schemes which are currently developed intensively.

We gratefully acknowledge fruitful discussions with F. F. Assaad, H. O. Jeschke, M. Knupfer, R. Kraus, A. M. Oleś, R. Valentí, and Y.-Z. Zhang. This work was supported by the Deutsche Forschungsgemeinschaft (DFG) under Grants CL124/6-1 and CL124/6-2.

-
- [1] N. F. Mott, Proc. Phys. Soc. London Sect. A **62**, 416 (1949).
 - [2] P. A. Lee *et al.*, Rev. of Mod. Phys. **78**, 17 (2006).
 - [3] A. Seidel *et al.*, Phys. Rev. B **67**, 020405(R) (2003).
 - [4] T. Saha-Dasgupta *et al.*, Europhys. Lett. **67**, 63 (2004).
 - [5] M. A. Hossain *et al.*, Nat. Phys. **4**, 527 (2008).
 - [6] H. Eskes *et al.*, Phys. Rev. Lett. **67**, 1035 (1991).
 - [7] D. C. Peets *et al.*, Phys. Rev. Lett. **103**, 087402 (2009).
 - [8] P. Phillips *et al.*, Phys. Rev. Lett. **105**, 199701 (2010).
 - [9] D. C. Peets *et al.*, Phys. Rev. Lett. **105**, 199702 (2010).
 - [10] H. Schäfer *et al.*, Z. Anorg. Allg. Chemie **295**, 268 (1958).
 - [11] See EPAPS Document No. [number will be inserted by publisher] for corresponding data.
 - [12] S. Yamanaka *et al.*, J. Mater. Chem. **19**, 2573 (2009).
 - [13] M. Sing *et al.*, Phys. Rev. Lett. **102**, 176805 (2009).
 - [14] Due to sample charging in PES, the energy axis was calibrated by extrapolating a temperature dependent series of spectra to zero charging. Hence we use the notation μ_{exp} for the position of the chemical potential.
 - [15] M. Imada *et al.*, Rev. Mod. Phys. **70**, 1039 (1998).
 - [16] H. Kajueter *et al.*, Phys. Rev. B **53**, 16214 (1996).
 - [17] M. Hoinkis *et al.*, Phys. Rev. B **75**, 245124 (2007).
 - [18] Y.-Z. Zhang *et al.*, Phys. Rev. Lett. **104**, 146402 (2010).
 - [19] J. S. Lee *et al.*, New J. Phys. **7**, 147 (2005).
 - [20] A. M. Oleś *et al.*, Phys. Rev. B **72**, 214431 (2005).
 - [21] R. Rückamp *et al.*, Phys. Rev. Lett. **95**, 097203 (2005).
 - [22] M. Hoinkis *et al.*, Phys. Rev. B **72**, 125127 (2005).
 - [23] C. A. Kuntscher *et al.*, Phys. Rev. B **74**, 184402 (2006).